



HAL
open science

Laboratory-Scale Bio-Treatment of Real Arsenic-Rich Acid Mine Drainage

Fabienne Battaglia-Brunet, Corinne Casiot, Lidia Fernandez-Rojo, Marina Hery, Pierre Le Pape, Hafida Tris, Guillaume Morin, Solène Touzé, Catherine Jouliau

► **To cite this version:**

Fabienne Battaglia-Brunet, Corinne Casiot, Lidia Fernandez-Rojo, Marina Hery, Pierre Le Pape, et al.. Laboratory-Scale Bio-Treatment of Real Arsenic-Rich Acid Mine Drainage. *Water, Air, and Soil Pollution*, 2021, 232 (8), pp.330. 10.1007/s11270-021-05276-z . hal-03365805

HAL Id: hal-03365805

<https://hal.science/hal-03365805v1>

Submitted on 5 Oct 2021

HAL is a multi-disciplinary open access archive for the deposit and dissemination of scientific research documents, whether they are published or not. The documents may come from teaching and research institutions in France or abroad, or from public or private research centers.

L'archive ouverte pluridisciplinaire **HAL**, est destinée au dépôt et à la diffusion de documents scientifiques de niveau recherche, publiés ou non, émanant des établissements d'enseignement et de recherche français ou étrangers, des laboratoires publics ou privés.

1 **Laboratory-scale Bio-treatment of Real Arsenic-rich Acid**

2 **Mine Drainage**

3 Battaglia-Brunet Fabienne^(*), Casiot Corinne, Fernandez-Rojo Lidia, Hery Marina, Le Pape
4 Pierre, Tris Hafida, Morin Guillaume, Touzé Solène, Joulian Catherine

5 F. Battaglia-Brunet (*), H. Tris, S. Touzé, C. Joulian: BRGM, Water, Environment, Process
6 Development and Analysis Division, 3 av. Claude Guillemin, BP 36009, 45060, Orléans Cedex
7 2, France

8 (*) e.mail: f.battaglia@brgm.fr ORCID 0000-0002-4005-6290

9 C. Casiot, L. Fernandez-Rojo, M. Hery: HydroSciences Montpellier, Univ Montpellier, CNRS,
10 IRD, Montpellier, France

11 P. Le pape, G. Morin: Institut de Minéralogie, de Physique des Matériaux et de Cosmochimie
12 (IMPMC), UMR 7590 CNRS-SU-IRD-MNHN, Sorbonne Université, case 115, 4 place Jussieu,
13 75252 Paris Cedex 05, France

14 **Abstract**

15 Acid mine drainage (AMD) still represents a huge environmental problem. Technical and
16 scientific breakthroughs are still needed to decrease environmental damages, treatment cost and
17 waste production associated with AMD. The feasibility of combining continuously fed
18 anaerobic sulfate-reducing bioreactor with downstream iron oxidation step was tested, at
19 laboratory scale, with two types of real arsenic rich AMD waters from the site of Carnoulès
20 (France), that differed in acidity (pH 3.3 and 4.0), arsenic (As, 18 and 174 mg/L) and metals
21 concentrations. Iron remained in solution while up to 99% of As was precipitated as amorphous
22 orpiment in the anaerobic sulfate-reducing bioreactor. Zinc (Zn) precipitation was also

23 observed, up to 99%, however the efficiency of Zn precipitation was less stable than that of As.
24 The anaerobic bioreactor presented a stable bacterial community including a
25 *Desulfosporosinus*-related sulfate-reducer. When the effluents from the anaerobic process step
26 were treated in a laboratory aerobic bioreactor, iron was oxidized efficiently. The feasibility of
27 efficient orpiment bio-precipitation coupled with downstream iron oxidation was shown, thus
28 opening the perspective of low-cost combination of treatment steps for the removal of arsenic,
29 zinc and iron in As-rich AMDs.

30 **Key words** arsenic, acid mine drainage, bioreactors, sulfate-reduction, bio-oxidation

31

32 **1 Introduction**

33 Acid mine drainage (AMD) causes extensive damage to the aquatic environment all around the
34 world (Simate and Ndlovu, 2014). This phenomenon affects many abandoned and remote sites,
35 where the application of the classical active lime treatment is technically and economically
36 problematic. Passive or semi-passive technologies have been developed, the global remediation
37 strategy generally involving several biological or physic-chemical treatment steps (Johnson and
38 Hallberg, 2005; Nairn et al., 2010; Mattes et al., 2011). Oxidation steps can be efficient to
39 remove iron (Fe), manganese (Mn), or co-precipitate Fe and arsenic (As) (Casiot et al., 2003;
40 Battaglia-Brunet et al., 2006; Wang et al., 2006; De Sa et al., 2010; Nairn et al., 2010;
41 Fernandez-Rojo et al., 2017, 2019). However, such aerobic processes are unsuitable for the
42 removal of divalent metal cations due to their poor sorption onto positively charged surface of
43 Fe-oxyhydroxides in acid conditions (Lee et al., 2002). On a complementary way, biological
44 reduction of sulfate efficiently removes metals such as zinc (Zn), copper (Cu), and lead (Pb) as
45 metallic sulfide precipitates and induces an increase of alkalinity and pH (Kaksonen and
46 Puhakka, 2007, Touzé et al., 2008). This treatment is also efficient to remove As (Mattes et al.,

2011), provided that low pH and/or low dissolved sulfide concentrations maintain sulfide amounts sufficiently low ($< 1 \text{ mg.L}^{-1}$) to avoid the formation of soluble thioarsenic species (Smieja and Wilkin, 2003). Sulfate reduction needs a costly supply in electron donor, such as hydrogen or organic molecules. To limit such costs, passive anaerobic bioreactors are generally filled with raw organic materials, such as agricultural, wood or food processing wastes which degradation provides electron donors for sulfate reduction (Parvis and Younger, 1999; Gibert et al., 2004; Mattes et al., 2011). However, in these systems, the sulfate-reducing activity cannot be regulated, all metals being precipitated as a bulk without selectivity. It would be interesting to regulate the activity of sulfate-reducing bacteria so as to remove only metals that cannot be eliminated, or only partially removed, in the aerobic steps. In this respect, iron sulfide (FeS) precipitation should be avoided since Fe can be efficiently treated in an oxidizing process (Fernandez-Rojo et al., 2017). Allocate the sulfate-reducing activity to the precipitation of a selection of metals will thus save organic substrate costs. Considering that FeS precipitates at pH higher than 5 (Kontopoulos, 1997), the sulfate-reducing bioreactor should be able to perform efficiently at lower pH. Sulfate reduction by acidophilic or acido-tolerant sulfate-reducing bacteria (SRB) has been reported as a promising way to remediate acid mine water while selectively precipitating metals as sulfides (Kimura et al., 2006; Johnson et al., 2009; Nancuqueo and Johnson, 2012; Nancuqueo et al., 2014; Sanchez-Andrea et al., 2015; Gonzales et al., 2019). The feasibility of As sulfide biosynthesis was demonstrated in batch laboratory bioreactors (Serrano and Leiva, 2017; Le Pape et al., 2017) or continuously fed with acidic (pH 2.5 to 4, Battaglia-Brunet et al., 2012; Altun et al., 2014) or mild acidic synthetic (pH 6-7, Rodriguez-Freire et al., 2014, 2015) solutions. Growth of SRB inducing precipitation of the orpiment and realgar, together with ZnS nanoparticles, has been proven in the real arsenic-rich acid mine water from Carnoulès site (France) in batch experiments (Le Pape et al., 2017).

71 Here, the two steps of a semi-passive process configuration including complementary anaerobic
72 and aerobic reactions were separately tested with the Carnoulès AMD in continuous laboratory-
73 scale bioreactors. These two complementary processes should allow removal of toxic metals
74 and high As contents from the AMD. Three main issues were addressed: (i) the feasibility of
75 orpiment precipitation from real arsenic-rich acidic mine water in an anaerobic SRB bioreator,
76 (ii) the separation of Fe, remaining in solution, from Zn and As, precipitated as sulfides, and
77 (iii) the aerobic bio-oxidation of remaining Fe present in the effluent from the anaerobic
78 bioreactor, and subsequent As removal.

79

80 **2 Materials and Methods**

81

82 **2.1 Mine waters**

83

84 AMD water was collected in July 2014 at the Carnoulès mine (Gard, France) from two different
85 springs: S1 and SSR, filtrated at 0.45 μm in a glovebox and stored at 5°C under nitrogen. NaOH
86 solution (1 M) was added to the water in a glovebox when pH adjustment was needed.
87 Characteristics of the water samples are given in Table 1. Among all metals and metalloids
88 present in these mine waters, As is particularly toxic, Zn is the most concentrated divalent metal,
89 and Fe is present at high level, close to 1 g.L^{-1} (le Pape et al., 2017).

90

91

92

93

94

95

96 2.2 Sulfate-reducing bioreactor

97

98 2.2.1 Experimental device

99

100 The sulfate-reducing bioreactor consisted of a 320 mm high and 35 mm internal diameter glass
101 column, equipped with a water jacket for temperature regulation. The bioreactor filling method
102 was conceived to: (1) test the passive distribution of nutrients to the bacteria, and (2) try to
103 establish different levels of SRB activities in the bottom and the top zones based on the
104 stimulation of SRB growth by yeast extract, thus testing the possibility to precipitate As in the
105 top layer (lower sulfate-reduction activity) and Zn in the bottom layer. The bioreactor (Fig. 1)
106 was filled in two distinct layers. For the top half of the bioreactor, pozzolana was mixed with
107 hot liquid agar (25 g.L^{-1}) prepared with deionized water acidified at pH 4.5 with H_2SO_4 ,
108 containing 5 g.L^{-1} glycerol and 0.5 g.L^{-1} K_2HPO_4 . After solidification of the agar, pozzolana
109 grains were separated using a spatula and mixed with a carrier biomaterial named
110 “biocompounds”, provided by Vertum GmbH (Walter et al., 2009) and composed of
111 polyhydroxybutyrate and polycaprolactone. The proportions of components were 160 g of
112 pozzolana / 100 g of biocompounds / 200 mL of agar with nutrients. The bottom filling material
113 had same composition except for the nutritive agar, supplemented with 1 g.L^{-1} yeast extract.
114 Sampling ports equipped with septa allowed liquid sampling from the middle, bottom and top
115 levels.

116 The bioreactor was inoculated with a sulfate-reducing microbial consortium, enriched from
117 sediments of the Carnoulès site. A basal medium (SM1) prepared at pH 3.5 and 4.5 was
118 supplemented with 327 mg.L^{-1} Zn and 75 mg.L^{-1} As(V) (using respectively 16 g.L^{-1} ZnSO_4
119 and 10 g.L^{-1} As(V) anaerobic stock solutions). Active cultures precipitating yellow-white
120 precipitates were sub-cultured in 40 mL basal medium supplemented with As and major metals

121 present in Carnoulès water: 2 mL of Fe(II) solution (final concentration 1 g.L⁻¹), 2 mL of metals
122 solution, 0.5 mL of As(III) solution (final concentration 100 mg.L⁻¹) and 0.2 mL of As(V)
123 solution (final concentration 40 mg.L⁻¹). Concentrated Fe(II) and metals solutions were
124 prepared under N₂ atmosphere, with oxygen-free ultrapure water acidified at pH 4.5 with
125 H₂SO₄. Fe(II) solution contained, per litre, 99.2 g of FeSO₄.7H₂O. Metals solution contained,
126 per litre: Al₂(SO₄)₃.18H₂O, 13.6 g ; MnSO₄.H₂O, 368 mg; NiSO₄.6 H₂O, 44 mg ; ZnSO₄.7H₂O,
127 1.77 g; CuSO₄.5 H₂O, 32 mg. Concentrated As(III) and As(V) solutions (10 g.L⁻¹ As) were
128 prepared as described in Battaglia-Brunet et al. (2002). Two sulfate-reducing cultures were
129 obtained after five sub-cultures at pH 3.5 and 4.5; they were mixed to obtain the sulfate-
130 reducing microbial consortium used to inoculate the bioreactor. A pellet of this inoculum was
131 stored at -20°C for DNA extraction and bacterial taxonomic identification.

132

133 2.2.2 Operating conditions

134

135 The bioreactor first worked in passive down-flow condition for 199 days, during which the
136 microbial activity was exclusively supported by the nutrients present in the solid filling
137 materials (Battaglia-Brunet et al., 2016). During this phase, the feed solution was a synthetic
138 mine water prepared adding the following components to 1 L deionized water whose pH was
139 adjusted with concentrated H₂SO₄: 2.3 g Na₂SO₄, 50 mL of Fe(II) solution, 50 mL of metals
140 solution, 10 mL of As(III) solution and 2.5 mL of As(V) solution. The pH dropped from 4.5 to
141 3.0 in 60 days. The present experiment started at Day 200, after this passive phase, using real
142 spring S1 mine water (pH 3.3) amended with 250 mg.L⁻¹ of glycerol as feed. The bioreactor
143 was down-flow fed during 26 days. Down-flow configuration consumes less energy than up-
144 flow however it increases the phenomena of preferential flow paths and clogging. Then, down-
145 flow was changed to up-flow feeding (day 226). At last, from day 315, the column was up-flow

146 fed with the spring SSR (pH 4.0) mine water complemented with 50 mg.L⁻¹ glycerol. The
147 temperature was maintained constant at 25°C.

148

149 2.2.3 Monitoring of the bioreactor

150

151 The outlet solution was collected and maintained under N₂ atmosphere. Once a day, the outlet
152 bottle was weighted to measure flow-rate. pH was measured and 5 mL of bioreactor outlet were
153 filtrated at 0.45 µm, acidified with nitric acid and stored at 5°C until As, Fe and Zn analyzes.
154 The remaining effluent was stored at 5°C under N₂ atmosphere until treatment in the aerobic
155 bioreactor. Feed was sampled once a week to check pH and chemical composition. Total As
156 was analyzed by oven AAS (Varian SpectrAA 220Z), Zn and Fe by flame AAS (VARIAN
157 SpectrAA 300). Total organic carbon was quantified by hot oxidation with sodium persulfate
158 (method NF EN 1484) and acetate was analyzed by ionic chromatography. Punctually (on days
159 201, 219, 288, 309 and 367), 5 mL of slurry were collected from top, middle and bottom septa
160 with a sterile syringe, filtrated on a sterile 0.22 µm cellulose acetate filter and the filters were
161 stored at -20°C for biomolecular analyzes. At the end of the experiment, the column was opened
162 in a glovebox under N₂ atmosphere. Samples of the filling material were stored at -20 °C for
163 biomolecular analyzes, and other samples were stored under N₂ for mineralogical analyzes.
164 After the bioreactor dismantling, “biocompound” particles were recovered, rinsed with
165 deionized water and dried at 40°C for 24 h then weighted to estimate the amount of consumed
166 material.

167

168 2.2.4 Composition of the inoculated sulfate-reducing consortium and evolution of the
169 bacterial community structure in the column

170 Microbial DNA was extracted from the -20°C stored samples, *i.e.* pellet of the inoculum, frozen
171 filters and filling materials (sampled at the end of the experiment), with the FastDNA Spin Kit
172 for soil applying a mechanical lysis at speed 5 during 30 s. Bacteria composing the inoculum
173 were identified by cloning and sequencing of the 16S rRNA gene. Briefly, about 1400 bp of the
174 gene were amplified from the extracted microbial DNA with primers 8F (5'-
175 AGAGTTTGATCMTGGCTCAG-3') and 1406R (5'-GACGGGCGGTGTGTRCA-3'), and
176 the purified PCR product was cloned into a PCR®4-TOPO vector, according to the
177 manufacturer instructions (Invitrogen). 32 plasmids carrying correct-length insert were
178 sequenced by the GATC company with primers T7 end T3 targeting the vector. Consensus
179 sequences were manually verified and aligned with ClustalW, and distances on unambiguous
180 nucleotide sequences were determined by DNADist, using applications implemented in the
181 BioEdit software (Hall, 1999). Operating taxon units (OTU) were built with retrieved sequences
182 sharing more than 98% identities. Distances between most related Genbank 16S rRNA gene
183 sequences of known bacteria, obtained by Blastn
184 (<http://www.ncbi.nlm.nih.gov/blast/Blast.cgi>), and defined OTU sequences were determined
185 by DNADist on 1372 aligned and unambiguous nucleotides. In addition, about 1.9 kb of the
186 *dsrAB* gene encoding the dissimilatory bisulfite reductase involved in reduction of sulfate, were
187 amplified with primers DSR1F (5'-ACSCAYTGGAARCACG-3') and DSR42R (5'-
188 GTGTARCAGTTDCCRCA-3'), cloned and sequenced as described. Consensus *dsrAB* gene
189 sequences sharing more than 98% identities by DNADist were grouped in OTU and compared
190 to Genbank reference sequences by Blastn. Most related reference and OTU *dsrAB* gene
191 sequences were translated into amino acids sequences, aligned and distances were calculated
192 by ProtDist (implemented in BioEdit software) on 552 unambiguous amino acids. Sequences
193 reported in this study are available under GenBank accession numbers MZ476566-MZ476597
194 (16S rRNA gene sequences) and MZ497397 to MZ497410 (*dsrAB* gene sequences).

195 The evolution of the structure of the bacterial community in the bioreactor was monitored by
196 16S rRNA gene CE-SSCP genetic fingerprints. About 200 bp of the V3 region of the bacterial
197 16S rRNA gene were amplified from DNAs (column samples and clones representing each
198 OTU from the inoculum) with the reverse primer w34 (5'-TTACCGCGGCTGCTGGCAC-3'),
199 5' end-labelled with the fluorescent dye FAM, and the forward primer w49 (5'-
200 ACGGTCCAGACTCCTACGGG-3'). Diluted PCR products (100 to 200 fold, to avoid
201 saturation of the fluorescent signal) were heat-denatured (95°C, 10 min) in HiDi Formamide
202 (Applied BioSystems) and submitted to a non-denaturing electrophoresis using the polymer
203 CAP and an ABI 310 genetic analyzer (Life Technologies), as already described (Battaglia-
204 Brunet et al., 2012). Internal DNA standard (Genescan 600-LYZ, Life Technologies) was used
205 to calibrate the runs. DNA fragments of 200 bp from columns' samples and inoculum clones
206 were run concomitantly in the same CE-SSCP capillary electrophoresis. Matching migration
207 pattern was used to assign a clone to a signal of the community patterns and determine if OTU
208 maintained or not in the column. Fingerprint profiles were aligned and compared with
209 BioNumerics version 7.6 software (Applied Maths).

210

211 2.2.5 Characterization of the precipitates

212

213 Black pouzzolana and yellow precipitate samples were analyzed using XRD. XRD
214 measurements were performed using a specifically designed anoxic cell with CoK α radiation
215 using a Panalytical X'Pert Pro diffractometer. Samples were grinded and suspended in ethanol
216 within an anaerobic chamber before being deposited on a Si single-crystal low-background
217 sample holder. Data were collected between 5 and 80° 2 θ with a 0.033° step, counting 2 hour
218 per sample. The yellow precipitate around pouzzolana grains was observed using electron
219 microscopy associated with microanalysis (SEM-EDXS analysis) on a GEMINI ZEISS Ultra55

220 Field Emission Gun Scanning Electron Microscope operating at 15 kV. Observations and
221 microanalysis were performed using backscattering electron signal and a Bruker QUANTAX
222 Energy dispersive X-ray spectrometer, respectively. For synchrotron based X-ray absorption
223 spectroscopy, the set of As-sulfide references considered in this study is detailed in Le Pape et
224 al. (2017). Briefly, experimental XAS spectra obtained on the column samples were compared
225 to the ones of amorphous orpiment (am-As₂S₃), crystalline orpiment (As₂S₃), and realgar (AsS),
226 minerals that are representative of an S-bound local molecular environment. As(V)- and
227 As(III)-sorbed ferrihydrites were used as reference compounds for O-bound local molecular
228 environment. As K-edge XANES and EXAFS spectra were collected at 15 K (He cryostat) in
229 both transmission and fluorescence mode on the SAMBA beamline (SOLEIL, France) using a
230 Si(220) double-crystal monochromator. Samples were always kept under inert atmosphere to
231 avoid oxidation. The incident energy was calibrated by measuring the LIII-edge of an Au foil
232 recorded in double transmission. Scans were averaged, normalized and background subtracted
233 using the Athena software. Linear combination fitting of XANES spectra were performed over
234 the -20 to 60 eV energy range.

235

236

237 2.3 Aerobic step

238

239 Effluents from the anaerobic bioreactor were treated in an aerobic bioreactor whose design was
240 described in Fernandez-Rojo et al. (2017b). Briefly, it was composed of 4 rectangular polyvinyl
241 chloride channels (1 m length × 0.06 m width × 0.06 m depth) equipped with a double envelope
242 for temperature regulation (20 ± 0.8 °C). One channel was used for the present experiment. A
243 canvas was placed on the bottom of the channel to provide a rough surface for the adhesion of
244 the biogenic precipitate. A peristaltic pump (Gilson, Minipuls 3) supplied the channel inlet with

245 AMD at a flow rate that determined the water residence time, here ~300 min. A second
246 peristaltic pump was necessary to pump the fluid out of the channel and to maintain the water
247 level at specific height (4 mm). A valve was positioned at the end of outlet tube for sample
248 collection. Prior to the treatment, a “conditioning” step was required to allow the development
249 of an active Fe-oxidizing biofilm. During this step, the aerobic bioreactor was fed with 0.5
250 mL.min⁻¹ of water S1, corresponding to a residence time (RT) of 324 ± 30 min. Inlet and outlet
251 water was collected at regular time intervals for dissolved Fe(II) and total dissolved Fe
252 determination until steady-state was reached with respect to Fe(II) oxidation. After steady-state
253 achievement (19 days), the channel was successively fed with (1) the anaerobically-treated
254 spring S1 water and (2) the anaerobically-treated spring SSR water. Efficiency of the aerobic
255 step was assessed by monitoring the inlet and outlet water chemistry. Analyzes included
256 measurement of pH, the determination of total concentrations of dissolved Fe(II) using
257 spectrophotometry, and total dissolved Fe, Zn and As using ICP-MS, after 0.2 µm filtration.
258 Arsenic redox speciation was determined using HPLC-ICP-MS. Details of these analytical
259 procedures are reported in Fernandez-Rojo et al. (2017).

260

261 **3 Results**

262

263 3.1 Anaerobic bioreactor

264

265 3.1.1 Evolution of physic-chemical parameters

266

267 During the down-flow feeding phase with spring S1, As removal efficiency averaged 64 ± 4 %
268 (157 mg.L⁻¹ As in the feed, 46 to 71 mg .L⁻¹ in the outlet) for a measured residence time of 298
269 ± 26 h (Fig. 2A and 2B) whereas within the same time, Zn removal (Fig. 2C) varied from 2 to

270 25% (24 mg.L^{-1} Zn in the feed, 16 to 23 mg.L^{-1} in the outlet) and Fe removal (Fig. 2D) from
271 10 to 30% (1270 mg.L^{-1} Fe in the feed, 84 to 1146 mg.L^{-1} in the outlet).

272

273 Substantial increase of Zn (Fig. 2C) concentration in the effluent after 208 days occurred
274 concomitantly to effluent pH decrease (Fig. 2E), consequence of clogging of the filling material
275 that resulted in disconnections of feeding pipe. The change (day 226) from down-flow to up-
276 flow configuration improved the efficiency of the bioreactor for As removal, that was higher
277 than 85% from day 245 to day 290 (Fig. 2B). As removal declined slightly with the decrease of
278 residence time from 300 h to 250 h after day 245 (event 1 on Fig. 2) but recovered at day 260.
279 The decrease of the mine water pH from 3.1 to 2.9 after day 270 (event 2 on Fig. 2) also induced
280 transient rise of As concentration in the outlet. A delay of 4-5 days was still observed between
281 the source of disturbance and the rise of As concentration in the outlet because of the high
282 residence time. After day 290, a new decrease in residence time from 250 h to 70 h (event 3 on
283 Fig. 2) induced a worsening of As removal that stabilized around 65%. Zn concentration
284 followed the same evolution as As but with variations of higher amplitude. The events that
285 affected As removal by 15% affected Zn removal by 90%. After day 290, the decrease of
286 residence time resulted in a very low level of Zn removal (less than 10%). During all the up-
287 flow feeding period, Fe was not removed (Fig. 2D). The pH always increased: while fed with
288 real mine water at pH close to 3, the pH in the outlet ranged from 4.3 to 4.8 (Fig. 2E).

289

290 Changing fed water from S1 to SSR corresponded to a decrease in Fe, Zn and As concentrations
291 and higher pH of the feed (event 4 on Fig. 2). After a transient period during which parameters
292 were influenced by the change of feed water quality, from day 312 to day 330, complete
293 removal of As and Zn was obtained. When the residence time in the bioreactor was

294 progressively decreased from 70 to 30 h (Fig. 1A), As and Zn were always almost entirely
295 removed from SSR water (Fig. 2B and 2C) and Fe was not precipitated (Fig. 2D).

296

297 Most of both As and Zn was precipitated in the bottom half of the column (Fig. SM2), so the
298 separation of As and Zn inside the column using different filling compositions was not
299 achieved. Acetate was always found in the outlet during the monitoring, however acetate
300 concentration in the outlet was 50% to 99% lower than the theoretical concentration that would
301 result from the incomplete oxidation of glycerol (Table SM3), except at the end of experiment
302 with spring SSR water, when the bioreactor was in a phase of degraded efficiency. At the end
303 of experiment, the visual appearance of the biocompounds and their weight did not differ
304 significantly from those of fresh biocompounds, suggesting they have not been biodegraded in
305 the bioreactor.

306 3.1.2 Composition of the inoculum and evolution of the bacterial community in the column

307 The 32 sequences of the 16S rRNA gene retrieved from the sulfate-reducing consortium
308 enriched from the Carnoulès site were classified into three OTU. The dominant OTU (90.6 %
309 of the sequences) shared 99.1 % identity on the 16S rRNA gene sequence with the acidophilic
310 sulfate-reducing bacterium *Desulfosporosinus* sp. PFB (Sen and Johnson, 1999). Another
311 *Desulfosporosinus*-related OTU represented 6.3 % of the sequences and showed more than 3 %
312 differences on the 16S rRNA gene with the dominant OTU; it shared 97.7 % and 97.8 % 16S
313 rRNA gene identities with *Desulfosporosinus* sp. OK and *Desulfosporosinus* sp. OL isolated
314 from an AMD (sequences available in Genbank under numbers MT359229 and MT359230).
315 The closest described *Desulfosporosinus* species most related (96-97 % identity) to these two
316 OTU were *D. lacus*, *D. meridiei*, *D. orientis*, *D. fructosivorans* and *D. auripigmenti*. The third
317 OTU grouping 3.1 % of the sequences was related (99.7 % 16S rRNA gene identity) to the

318 *Propionibacteraceae* strain H7p isolated from Carnoulès acid mine drainage (Delavat et al.,
319 2012); except for its tolerance to low pH, no data is currently available on its metabolism.

320 Sixteen dissimilatory bisulfite reductase (DsrAB) sequences retrieved from the inoculum
321 formed two related OTU sharing 97.4 % identity on their DsrAB aminoacids sequences. The
322 closely related (85.6 % identity) DsrAB sequence to both OTU belonged to the acidophilic
323 *Desulfosporosinus* sp. DB isolated from an AMD (Karnachuk et al., 2009), and the closest
324 described species were *Desulfosporosinus adidiphilus*, *D. acididurans* and *D. meridiei* with
325 respectively 76.5 %, 75.7 % and 72.3 % identities. These results are in line with those obtained
326 from 16S rRNA gene sequence analyzes, and confirm that sulfate-reducing strains belonging
327 to the *Desulfosporosinus* genus are present in the sulfate-reducing inoculum enriched from
328 Carnoulès site.

329 The evolution of fingerprints of the bacterial community sampled during time and location in
330 the column are presented in Fig. 3. Fingerprints were quite similar at the top, middle and bottom
331 of the column, showing a homogeneous distribution of the bacteria in the bioreactor. At days
332 288 and 309, the structure of the community has evolved and only two of the peaks detected at
333 day 219 remained largely dominant. Changes in operating conditions, *i.e.* upflow fed and pH
334 decrease from 3.1 to 2.9, may have favored the corresponding bacteria. The change from spring
335 S1 to SSR site water from day 309 to the end of the monitoring (day 367) did not affect much
336 the structure of the community at the top and bottom location, while more peaks were detected
337 at the middle location. The signal corresponding to the *Desulfosporosinus* OTU initially
338 dominant in the sulfate-reducing inoculum, which was also present during the previous stage
339 of feeding with synthetic mine water (Battaglia-Brunet et al., 2016), was one of the dominant
340 throughout the monitoring. Its presence regardless of the condition applied to the column
341 emphasizes its ability to maintain itself under the different conditions applied to the column, in
342 particular a pH of 3 of the feed water. It was also found on the filling material sampled at the

343 end of the monitoring (data not shown), confirming its presence in the biofilm attached on the
344 solid support. No signal corresponding to the *Propionibacteraceae* bacterium found in the
345 inoculum was evidenced, indicating that its proportion amongst other bacteria represented, if
346 present, only as a small fraction of the total community.

347 3.1.3 Characterization of the precipitates

348 In the samples from the column, *i.e.* black pouzzolana and yellow precipitate, analyzed using
349 XRD (Fig. SM4-A), no As-bearing phase was observed. The composition is in line with usual
350 mineral compounds used in pouzzolana, *e.g.* feldspars. In the yellow precipitate recovered
351 around the pouzzolana grains, only gypsum was observed as crystalline material. However,
352 very low amplitude reflexions as well as large bumps above the background suggest the
353 presence of amorphous or nanocrystalline materials.

354

355 Both XANES and EXAFS spectra obtained at the As K-edge for the different samples collected
356 in the column were compared to reference materials representative for specific As local
357 molecular environments. Realgar (AsS) and amorphous orpiment (am-As₂S₃) were used as
358 references for sulfur bound As, and As(III)-sorbed ferrihydrite and As(V)-sorbed ferrihydrite
359 were used as proxies of oxygen bound As. Linear combination fitting analysis performed on As
360 K-edge XANES spectra shows that the samples mainly contained amorphous orpiment (89 to
361 100 %) and a minor amount of oxygen bound As(III) (0 to 13 %) (Fig. SM4-B and Table SM4-
362 C). Even considering the low quality of EXAFS signal for some of the samples (Fig. SM4-D),
363 both EXAFS oscillations and Fast Fourier Transform confirm the major occurrence of
364 amorphous orpiment in the samples recovered from the column experiment (Fig. 4). As both
365 XANES and EXAFS spectra of thiol-bound As(III) are difficult to differ from the one of
366 amorphous orpiment, the presence of such As species cannot be excluded in the samples. In

367 addition, the presence of minor amount of oxygen bound As(V) and realgar (< 5%) cannot be
368 discarded considering the standard uncertainty of XAS-LCF analysis.

369

370 In Fig. 4, the image of yellow precipitate was taken in backscattering electron mode, thus the
371 brightest spots indicate the presence of the heaviest elements. In this particular case, the
372 brightness of particles is related to the As content. Both encrusted and non-encrusted bacteria
373 are observed, as well as submicrometric aggregates of spherical particles connected or not with
374 bacteria. All the particles probed using EDXS (1 to 6, Fig. 4) showed a major signal of As and
375 S, which is consistent with arsenic sulfides as the main products of the sulfate-reducing activity
376 of the biofilm. Only traces of Fe and Zn were detected in the EDXS spectra, confirming that As
377 was the main element to precipitate as biogenic sulfide in the bioreactor. In addition to the large
378 occurrence of aggregates of spherical nanoparticles in the biofilm, nanospheres can be observed
379 on the surface of bacterial cells (Fig. 4A). This observation would be consistent with those of
380 Newmann (1997) who observed the extracellular precipitation of orpiment nanoparticles on
381 sulfate-reducing bacteria mineralizing arsenic.

382

383 3.2 Coupling with aerobic step

384

385 The aerobic step was tested as a preliminary evaluation of the feasibility of biological oxidation
386 of Fe(II) and increase of As removal in the sulfate-reduction bioreactor effluent, that contained
387 also organic substances, potentially inhibitors of Fe(II) and As(III) bio-oxidation. This
388 treatment induced a decrease of pH and Fe concentration: 7% (S1) and 9% (SSR) removal were
389 obtained within 300 minutes (Fig. 5). Concerning As, for spring S1, nearly 90% removal was
390 obtained in the anaerobic bioreactor, and the aerobic step improved the overall removal,
391 decreasing both As(III) and As(V) concentrations by 33% and 44%, respectively. These results

392 represent a gain of 6% removal for As(III) and 4% for As(V) considering the initial composition
393 of the mine water. Conversely, with spring SSR, the aerobic step did not induce any As removal.
394 Surprisingly, a release of As(III) was observed in these conditions. The aerobic step had no
395 effect on Zn concentration.

396

397 **4 Discussion**

398

399 Up to now, laboratory continuous experiments dedicated to the biological precipitation of
400 arsenic sulfide were fed with synthetic solutions (Battaglia-Brunet et al., 2012; Altun et al.,
401 2014; Rodriguez-Freire et al., 2014, 2015). Here, a real As-rich acidic mine water, of complex
402 composition, was used to confirm the feasibility of continuous anaerobic precipitation of
403 orpiment at low pH, in accordance with batch experiment data (Le Pape et al., 2017). The
404 present experiment with real mine water and glycerol supply started on day 200, after the
405 bioreactor was fed with synthetic mine water during 199 days under entirely passive conditions
406 (Battaglia-Brunet et al., 2016). During this previous experimental phase, a progressive decrease
407 of the bioreactor efficiency had been observed, linked to the exhausting of substrates initially
408 placed into the column. Semi-passive sulfate-reducing bioreactors are increasingly seen as a
409 viable option for highly contaminated AMD (Lounate et al., 2020). One of the objectives of the
410 present study was to evaluate the precipitation of As and Zn in the sulfate-reducing bioreactor
411 working in semi-passive condition, while Fe remained in solution, knowing that: (1) As is toxic
412 and cannot be valorized, thus should be precipitated in the smallest volume of waste as possible,
413 (2) Zn must be removed during the sulfate-reducing step because the oxidation step will not
414 remove it, (3) Fe can be efficiently removed downstream by passive microbial or chemical
415 oxidation step, co-precipitating the residual As. Furthermore, as Fe is the most concentrated

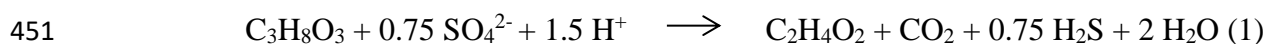
416 metal in Carnoulès AMD, avoiding its precipitation in the anaerobic bioreactor will save
417 organic substrates and prevent rapid clogging.

418 The theoretical mass balance comparing our process configuration with a classical lime
419 treatment directly applied to the spring S1 AMD (Fig. 6) suggests that the amount of As-
420 contaminated solid waste could be drastically decreased applying a sulfate-reduction step
421 followed by aerobic oxidation. Moreover, the classical lime application could not remove Zn
422 from water unless reaching pH 9.5 (Murdock et al., 1993), thus implying a supplementary final
423 step of acid addition.

424 The direct feeding of sulfate-reducing bacteria with the acid mine waters S1 et SSR was
425 possible, in spite of the low pH, because iron, although present in high concentration, is mainly
426 under the Fe(II) form in Carnoulès water (Casiot et al., 2003). The sulfate reduction induced an
427 increase of one unit pH along the experiment. However, the pH in the outlet remained acidic,
428 contrary to previous studies (Battaglia-Brunet et al., 2012; Altun et al., 2014; Rodriguez-Freire
429 et al., 2014, 2015), where the electron donor was not limiting, supporting an extended sulfate-
430 reduction activity and resulting in a pH value higher than pH 5-6 in the outlet. Here, the
431 moderate pH increase, linked to the limited substrate supply, allowed separating Fe, that
432 remained in solution, from Zn and As that were precipitated together during periods of efficient
433 microbial activity. However, the anaerobic bioreactor was more efficient to remove As than Zn:
434 the weakening of bacterial activity always affected Zn precipitation more than As removal
435 during the experiment with spring S1. Precipitation of amorphous orpiment is favored at low
436 pH (Eary, 1992): the more acid the medium is, the more orpiment precipitation is efficient.
437 With spring S1 water, le Pape et al. (2017) already showed that As precipitation was more rapid
438 than that of Zn. With spring SSR, the feed pH (pH 4) was already higher than the value
439 necessary for ZnS precipitation, that could explain the efficient removal of both Zn and As from
440 this mine water. Mattes et al. (2011) already reported efficient removal of both As and Zn from

441 a smelter landfill seepage (pH 5.9), through a real scale anaerobic passive bioreactor filled with
442 a mixture of limestone, quartz sand and organic waste.
443 Here, considering that production of sulfide was mainly coupled to incomplete degradation of
444 glycerol (reaction 1), and consumption of sulfide occurred according to reactions (2) and (3),
445 the total amount of glycerol necessary to precipitate all As (2 mM) and Zn (0.3 mM) present in
446 S1 should be 4.4 mM, *i.e.* 405 mg L⁻¹. Yet, the bioreactor feed contained only 250 mg L⁻¹
447 glycerol, a limiting concentration that should not have been sufficient for the precipitation of
448 both As and Zn, whereas the complete removal of these two elements was observed during
449 some periods of the experiment.

450



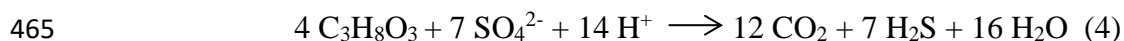
452



454



456 This result may be explained by the complete oxidation of glycerol, according to reaction (4),
457 that would produce 2.3 times more H₂S than reaction (1). As a fact, acetate concentration in the
458 bioreactor outlet was lower than the theoretical concentration corresponding to the incomplete
459 oxidation of all the glycerol supplied with the feed water. Nancucheo and Johnson (2014)
460 already observed a decrease of acetate concentration in a sulfate-reducing bioreactor fed with
461 glycerol, when the working pH was decreased from 4.5 to 3.0. The switch from incomplete to
462 complete oxidation of glycerol was accompanied by a change in the bacterial community
463 structure. The solid filling material, initially loaded with agar, yeast extract and glycerol, could
464 also slowly release organic molecules that played the role of complementary electron donors.



466 Initially, the bioreactor was inoculated with a sulfate-reducing consortium mainly composed
467 SRB affiliated to the *Desulfosporosinus* genus. Two distinct OTU were retrieved; they showed
468 less than 97 % sequence identity on their 16S rRNA genes, and 96-97 % identities with
469 described *Desulfosporosinus* species (*D. lacus D. meridiei*, *D. orientis*, *D. fructosivorans* and
470 *D. auripigmenti*). If we consider a cut-off value at the species level of 98.7% or above on the
471 16S rRNA gene (Rossi-Tamisier et al., 2015), the two-retrieved OTU may represent new
472 acidophilic species of the *Desulfosporosinus* genus. The OTU sequences had higher identity
473 values with yet undescribed acidophilic isolates of the genus: 99 % between the dominant OTU
474 and *Desulfosporosinus* sp. PFB (Sen and Johnson, 1999) and 98 % between the second SRB
475 OTU and *Desulfosporosinus* sp. OK and OL (MT359229 and MT359230 Genbank accession
476 numbers). The *Desulfosporosinus* genus comprises several members known to reduce sulfate,
477 in acidic conditions, and often isolated from mining sites (*e.g.* Sen and Johnson, 1999;
478 Karnachuk et al., 2009; Alazard et al., 2012; Sánchez-Andrea et al., 2015). All these
479 *Desulfosporosinus* strains are incomplete oxidizers using glycerol to reduce sulfate and produce
480 acetate. Based on community fingerprints, one of the SRB OTU was among the dominant
481 microorganism in the bioreactor, all along the experiment. *Desulfosporosinus*-like 16S
482 sequences were already detected in bioreactors treating As-containing acid solutions (Battaglia-
483 Brunet et al., 2012) and Gonzales et al. (2019) observed a SRB affiliated to *Desulfosporosinus*
484 *acididurans* becoming dominant in their bioreactor treating a synthetic AMD in continuous
485 mode. Moreover, analysis of microbial communities revealed the widespread presence of
486 *Desulfosporosinus*-related sulfate reducers in diverse SRB reactors treating AMD from
487 laboratory to real scale (Habe et al., 2020).

488 In the present study, mineralogical observations of the precipitates formed in the bioreactor
489 were globally in line with those obtained from batch experiments, with AMD from the same

490 site, in comparable conditions (Le Pape et al., 2017). However, if the major occurrence of
491 amorphous orpiment is strongly suspected from SEM-EDXS and confirmed by XANES and
492 EXAFS spectroscopy, no realgar was detected in the form of nanowires in the biofilm observed
493 by SEM-EDXS. Thus, the processes occurring within the continuous column experiment would
494 be representative of the early stages of As reduction and precipitation processes identified in
495 the batch experiment system, before reduction of orpiment into realgar (Le Pape et al., 2017).

496

497 When the outlet water from the anaerobic reactor was treated in aerobic condition, partial
498 oxidation of iron and a decrease of pH were observed. The iron removal rate with S1 and SSR
499 waters were 1.1×10^{-7} and $0.9 \times 10^{-7} \text{ mol.L}^{-1}.\text{s}^{-1}$ respectively, that is of the same range but lower
500 than the iron removal rates previously reported during direct aerobic treatment of this AMD in
501 the same reactor ($1.3 - 2.4 \times 10^{-7} \text{ mol.L}^{-1}.\text{s}^{-1}$, Fernandez-Rojo et al., 2017). The hydraulic
502 residence time was only 300 min, so largely lower than that applied in the anaerobic step. The
503 conditions of this aerobic step remain to be optimized. Gonzales et al. (2019) observed the
504 complete oxidation of the ferrous iron present in the outlet of a SRB bioreactor, corresponding
505 to nearly 1 mM, in 1 h aeration. Here, some As was removed from S1 water previously treated
506 anaerobically, however with SSR water, some release of As(III) occurred. This phenomenon
507 may be linked to the sharp shift from S1 to SSR water compositions, inducing a decrease of As
508 concentration in the feed (17 to 3 mg L^{-1} respectively), and might be linked to the sorption-
509 desorption equilibrium of As(III) associated with the iron precipitates, or to the solubility of
510 As(III)-shwermannite accumulated in the reactor during the previous step. A decrease of
511 As(III)-oxidation activity might also have occurred. The activity of As(III)-oxidizing bacteria
512 may be influenced by the residual organic molecules from the anaerobic reactor. As(III)-
513 oxidizing bacteria can grow heterotrophically or autotrophically (Santini et al., 2000; Battaglia-
514 Brunet et al., 2006; Garcia-Dominguez et al., 2008). In particular, strains of *Thiomonas*, the

515 main As(III)-oxidizing genus found in Carnoulès AMD (Hovasse et al., 2016), are facultative
516 chemolithoautotrophs that grow optimally in mixotrophic media containing reduced inorganic
517 sulfur compounds and organic supplements (Bryan et al., 2009; Slyemi et al., 2011). Tardy et
518 al. (2018) observed a stimulation of As(III)-oxidation by yeast extract, in the AMD of Carnoulès
519 mine. However, the effect of organic substrates might depend on the nature of the supplied
520 molecules: how the bacterial communities of the biofilms inside the aerobic channel are
521 impacted by the anaerobic effluent would require further analyzes.

522 **5 Conclusions**

523 The feasibility of arsenic precipitation as orpiment in a sulfate-reducing bioreactor fed with two
524 types of real As-rich mine drainage waters was demonstrated at laboratory scale. Limitation of
525 sulfate-reduction by low supply of carbon and energy source allowed the removal of most
526 arsenic while iron remained in the water. Precipitation of zinc in the sulfate-reducing reactor
527 was efficient with the low-concentrated AMD, whereas optimization is still needed in order to
528 stabilize this process with the most concentrated AMD. The separation of arsenic from iron in
529 such type of mine water may be beneficial in terms of most hazardous waste mass, as the main
530 part of the arsenic would be concentrated as As_2S_3 . The net consumption of glycerol for a given
531 As and Zn removal could be lower than initially expected because this substrate can be entirely
532 and not incompletely degraded. Downstream oxidation and precipitation of iron, besides
533 additional As removal, was proven to occur in an aerobic laboratory bioreactor, although not
534 optimized in the present study. Whereas the two treatment steps studied here allowed the
535 removal of 70 to 95% of As, in two different AMD streams, a down-stream lime drain would
536 be necessary in order to increase the final pH of the treated water, and remove the residual As
537 and Fe by co-precipitation. Results support the feasibility of applying simple combination of
538 low-cost treatment options, including semi-passive SRB bioreactor, for the remediation of As-
539 rich AMDs.

540

541 **Declarations**

542 **Funding** This research was financially supported by the French ANR (Agence Nationale de la
543 Recherche) in the frame of IngECOST-DMA project (ANR-13-ECOT-0009).

544 **Conflict of Interest** The authors declare they have no conflict of interest.

545 **Availability of data and material** All data are available on request to the corresponding author
546 (e.mail: f.battaglia@brgm.fr)

547 **Authors contribution** F. Battaglia-Brunet: Conceptualization, Writing, Supervision; L.
548 Fernandez-Rojo: Investigation, Editing; M. Hery: Editing; C. Casiot: Conceptualization,
549 Methodology, Supervision, Writing, Editing; P. Le Pape: Investigation, Writing, Editing; H.
550 Tris: Investigation; S. Touzé: Conceptualization; G. Morin: Supervision, Editing; C. Joulian:
551 Investigation, Supervision, Writing, Editing.

552

553 **Figure captions**

554 **Figure 1.** Bioreactor filling and feeding modes, down-flow (A), up-flow (B), and pictures taken
555 just after filling (C) and at the end of experiment (D).

556

557 **Figure 2.** Evolution of parameters in the bioreactor fed with springs S1 then SSR mine water.

558 A: residence time (h), B: arsenic concentration (mg.L^{-1}), C: zinc concentration (mg.L^{-1}), D: iron
559 concentration (mg.L^{-1}), E: pH. Numbered vertical lines show specific events: (1) and (3)
560 decrease of residence time; (2) decrease in feed pH, (4) change from spring S1 to spring SSR.

561 The pH value increased from 4.0 in the feed to 4.5-5.0 in the outlet, except during the last days
562 of experiment, probably because of the decrease of residence time from 40 to 30 h (Fig. 2E).

563

564 **Figure 3.** Evolution of 16S rRNA gene CE-SSCP fingerprints at the bottom (B), mid (M) and
565 top (T) of the column. *: signal matching with the signal of the *Desulfosporosinus* OTU
566 originally dominant in the inoculated bacterial mixed culture. Horizontal scale: migration
567 position of detected signals determined from electrophoretic scans.

568

569 **Figure 4.** Analysis of As mineralogy and speciation in yellow deposits that precipitated at the
570 surface of pouzzolana grains in the column experiment. (A) SEM image in backscattering
571 electron mode showing the biofilm morphology. Plain orange arrows indicate mineralized
572 encrusted bacterial cells; dashed orange arrows indicate non-mineralized cells; Blue arrows
573 indicate aggregates of spherical nanoparticles. (B) Microanalyses performed using Energy
574 dispersive X-Ray spectroscopy (EDXS) at different spots of approximately $1\mu\text{m}^3$ on the biofilm
575 sample (spots 1 to 6 in red on the image). The emission spectra 1 to 6 show the presence of As
576 and S as main constitutive elements (C) XANES spectra and (D) EXAFS spectra of the bulk
577 sample (black) and of amorphous orpiment reference sample (red). Bulk solid speciation of As
578 in the biofilm is similar to that of amorphous orpiment (E) Fast Fourier transform of the EXAFS
579 signal. Additional data relative to XAS analysis for different samples of the column are
580 available in SM4 (Figures SM4B and SM4D, and Table SM4C).

581

582

583

584 **Figure 5.** Evolution of S1 (A) and SSR (B) water parameters before treatment, after the
585 anaerobic step (SRB) and in the outlet of the aerobic step (OX).

586

587 **Figure 6.** Theoretical mass balance for the treatment of spring S1 AMD by a SRB bioreactor
588 coupled with acidic aerobic step followed by lime addition, compared with simple one-step
589 lime treatment. The percentage of Fe removal as schwertmannite by acidic oxidation is inspired
590 by previous results of Fernandez-Rojo et al. (2017); (a) analytical quantification limit; (b)
591 formula according to Garcia-Rios et al. (2021); (c) solubility of gypsum according to Lebedev
592 and Kosorukov (2017).

593

594 **References**

595 Alazard, D., Joseph, M., Battaglia-Brunet, F., Cayol, J.-L., Ollivier, B. (2012).
596 *Desulfosporosinus acidiphilus* sp. nov.: a moderately acidophilic sulfate-reducing bacterium
597 isolated from acid mining drainage sediments. *Extremophiles*, 14, 305–312.

598 Altun, M., Sahinkaya, E., Durukan, I., Bektas, S., Komnitsas, K. (2014). Arsenic removal in a
599 sulfidogenic fixed-bed column bioreactor. *Journal of Hazardous Materials*. 269, 31-37.

600 Battaglia-Brunet, F., Dictor, M.-C., Garrido, F., Crouzet, C., Morin, D., Dekeyser, K., Clarens,
601 M. & Baranger, P. (2002). An arsenic(III)-oxidizing bacterial population: selection,
602 characterization and performance in reactors. *Journal of Applied Microbiology*, 93(4), 656-667.

603 Battaglia-Brunet, F., Itard, Y., Garrido, F., Delorme, F., Crouzet, C., Greffie, C., Jouliau, C.
604 (2006). A simple biogeochemical process removing arsenic from a mine drainage water.
605 *Geomicrobiology Journal*, 23(3-4), 201–211.

606 Battaglia-Brunet, F., Crouzet, C., Burnol, A., Coulon, S., Morin, D., Jouliau, C. (2012).
607 Precipitation of arsenic sulphide from acidic water in a fixed-film bioreactor. *Water Research*
608 46(12), 3923-3933.

609 Battaglia-Brunet, F., Jouliau, C., Casiot, C. (2016). Development of a passive bioremediation
610 process based on sulfate-reduction to treat arsenic-containing acidic mine water. In P.
611 Bhattacharya, M. Vahter, J. Jarsjö, J. Kumpiene, A. Ahmad, C. J. Sparrenbom, G. Jacks, M. E.
612 Donselaar, J. Bundschuh, R. Naidu (Eds), *Arsenic Research and Global Sustainability: Proceedings of the Sixth International Congress on Arsenic in the Environment (As2016)*, CRC
613 Press/Balkema, 2016. 730 p.

615 Bryan, C. G., Marchal, M., Battaglia-Brunet, F., Kugler, V., Lemaitre-Guillier, C., Lièvreumont,
616 D., et al. (2009). Carbon and arsenic metabolism in *Thiomonas* strains: differences revealed
617 diverse adaptation processes. *BMC Microbiology*, 9, 127.

618 Casiot, C., Morin, G., Juillot, F., Bruneel, O., Personné, J.-C., Leblanc, M., Duquesne, K.,
619 Bonnefoy, V., Elbaz-Poulichet, F., (2003). Bacterial immobilization and oxidation of arsenic
620 in acid mine drainage (Carnoulès creek, France). *Water Research*, 37(12), 2929–2936.

621 Delavat, F., Lett, M.-C., Lièvreumont, D. (2012). Novel and unexpected bacterial diversity in an
622 arsenic-rich ecosystem revealed by culture-dependent approaches. *Biology Direct*, 7, 28.

623 DeSa, T., Brown, J., Burgos, W. (2010). Laboratory and field-scale evaluation of low-pH Fe(II)
624 oxidation at Hughes Borehole, Portage, Pennsylvania. *Mine Water and the Environment*, 29,
625 239–247.

626 Eary, L. E. (1992). The solubility of amorphous As_2S_3 from 25 to 90°C. *Geochimica et*
627 *Cosmochimica Acta*, 56(6), 2267-2280.

628 Fernandez-Rojo, L., Hery, M., Le Pape, P., Braungardt, C., Desoeuvre, A., Torres, E., Tardy,
629 V., Resongles, E., Laroche, E., Delpoux, S., Jouliau, C., Battaglia-Brunet, F., Boisson, J.,
630 Grapin, G., Morin, G., Casiot, C. (2017). Biological attenuation of arsenic and iron in a
631 continuous flow bioreactor treating acid mine drainage (AMD). *Water Research*, 123, 594-606.

632 Fernandez-Rojo, L., Casiot, C., Laroche, E., Tardy, V., Bruneel, O., Delpoux, S., Desoeuvre,
633 A., Grapin, G., Savignac, J., Boisson, J., Morin, G., Battaglia-Brunet, F., Jouliau, C., Hery, M.
634 (2019). A field-pilot for passive bioremediation of As-rich acid mine drainage. *Journal of*
635 *Environmental Management*, 232, 910-918.

636 Garcia-Dominguez, E., Mumford A., Rhine, E D., Paschal, A., Young, L. Y. (2008). Novel
637 autotrophic arsenite-oxidizing bacteria isolated from soil and sediments. *FEMS*
638 *Microbiology Ecology*, 66(2), 401–410.

639 Garcia-Rios, M., De Windt, L., Luquot, L., Casiot, C. (2021). Modeling of microbial kinetics
640 and mass transfer in bioreactors simulating the natural attenuation of arsenic and iron in acid
641 mine drainage. *Journal of Hazardous Materials*, 405, 124133.

642 Gibert, O., de Pablo, J., Cortina, J. L., Ayora, C. (2004). Chemical characterisation of natural
643 organic substrates for biological mitigation of acid mine drainage. *Water Research* 38(19),
644 4186–4196.

645 Gonzalez, D. Liu, Y., Villa Gomez, D., Southam, G., Hedrich, S., Galleguillos, P., Colipai, C.,
646 Nancucheo, I. (2019). Performance of a sulfidogenic bioreactor inoculated with indigenous
647 acidic communities for treating an extremely acidic mine water. *Minerals Engineering*, 131,
648 370-375.

649 Habe, H., Sato, Y., Aoyagi, T., Inaba, T., Hori, T., Hamai, T., Hayashi, K., Kobayashi, M.,
650 Sakata, T., Sato, N. (2020). Design, application, and microbiome of sulfate-reducing

651 bioreactors for treatment of mining-influenced water. *Applied Microbioly and Biotechnoly*, 104,
652 6893–6903.

653 Hall, T. A. (1999). BioEdit: a user-friendly biological sequence alignment editor and analysis
654 program for Windows 95/98/NT. *Nucleic Acids Symposium Series*, 41, 95-98.

655 Hovasse, A., Bruneel, O., Casiot, C., Desoeuvre, A., Farasin, J., Hery,, M., Van Dorsselaer, A.,
656 Carapito, C., Arsène-Ploetze, F. (2016). Spatio-temporal detection of the *Thiomonas* Population
657 and the *Thiomonas* arsenite oxidase involved in natural arsenite attenuation processes in the
658 Carnoulès acid mine drainage. *Frontiers in Cell and Developmental Biology*, 4, 3.
659 www.frontiersin.org/article/10.3389/fcell.2016.00003

660 Johnson, D. B., Jameson, E., Rowe, O. F., Wakerman, K., Hallberg, K. B. (2009).
661 Sulfidogenesis at low pH by acidophilic bacteria and its potential for the selective recovery of
662 transition metals from mine waters. *Advanced Materials Research*, 71-73, 693-696.

663 Kaksonen, A. H., Puhakka, J. A. (2007). Sulfate reduction based bioprocesses for the treatment
664 of acid mine drainage and the recovery of metals. *Engineering in Life Sciences*, 7(6), 541–564.

665 Karnachuk, O. V., Gerasimchuk, A. L., Banks, D., Frengstad, B., Stykon, G. A., Tikhonova, Z.
666 L., Kaksonen, A., Puhakka, J., Yanenko, A. S., Pimenov, N. V. (2009). Bacteria of the sulfur
667 cycle in the sediments of gold mine tailings, Kuznetsk Basin, Russia. *Microbiology*, 78, 483-
668 491.

669 Kimura, S., Hallberg, K. B., Johnson, D. B. (2006). Sulfidogenesis in low pH (3.8-4.2) media
670 by a mixed population of acidophilic bacteria. *Biodegradation*, 17, 159-167.

671 Kontopoulos, A. (1997). Effluent treatment in the mining industry. S.H. Castro, F. Vegara, and
672 M. A. Sanchez (Eds), University of Concepcion-Chile.

673 Lebedev, A. L., Kosorukov, V. L. (2017). Gypsum Solubility in Water at 25°C. *Geochemistry*
674 *International*, 55(2), 205–210.

675 Lee, G., Bigham, J. M., Faure, G. (2002). Removal of trace metals by coprecipitation with Fe,
676 Al and Mn from natural waters contaminated with acid mine drainage in the Ducktown Mining
677 District, Tennessee. *Applied Geochemistry*, 17(5), 569-581.

678 Murdock, D. J., Fox, J. R. W., Bensley, J. G. (1993). Treatment of acid mine drainage by the
679 high density sludge process. *Proceedings America Society of Mining and Reclamation*, pp. 241-
680 249.

681 Le Pape, P., Battaglia-Brunet, F., Parmentier, M., Jouliau, C., Gassaud, C., Fernandez-Rojo, L.,
682 Guigner, J.-M., Ikogou, M., Stetten, L., Olivi, L. Casiot, C., Morin, G. (2017). Complete
683 removal of arsenic and zinc from a heavily contaminated Acid Mine Drainage via an indigenous
684 SRB consortium. *Journal of Hazardous Materials*, 321, 764-772.

685 Lounate, K., Coudert, L., Genty, Mercier, G., Blaise, J.-F. (2020) Performance of a Semi-
686 passive Sulfate-reducing Bioreactor for Acid Mine Drainage Treatment and Prediction of
687 Environmental Behavior of Post-treatment Residues. *Mine Water and the Environment*, 39,
688 769–784.

689 Mattes, A., Evans, L. J., Gould, W. D., Duncan, W. F. A., Glasauer, S. (2011). The long term
690 operation of a biologically based treatment system that removes As, S and Zn from industrial
691 (smelter operation) landfill seepage. *Applied Geochemistry*, 26(11), 1886-1896.

692 Nairn, R. W., LaBar, J.A., Strevett, K. A., Strosnider, W. H., Morris, D., Neely, C. A., Garrido,
693 A., Santamaria, D., Oxenford, L., Kauk, K., Carter, S., Furneaux, B. (2010). A large, multi-cell,
694 ecologically engineered passive treatment system for ferruginous lead-zinc mine waters. In

695 Wolkersdorfer & Freund (Eds), Mine Water and Innovative Thinking, Proceedings of the
696 IMWA 2010, pp. 255-258.

697 Nancucheo, I., Johnson, D. B. (2012). Selective removal of transition metals from acidic mine
698 waters by novel consortia of acidophilic sulfidogenic bacteria. *Microbial Biotechnology*, 5, 34–
699 44.

700 Nancucheo, I., Johnson, D. B. (2014). Removal of sulfate from extremely acidic mine waters
701 using low pH sulfidogenic bioreactors. *Hydrometallurgy*, 150, 222-226.

702 Parvis, A. P., Younger, P. L. (1999). Design, construction and performance of a full-scale
703 compost wetland for mine-spoil drainage treatment at quaking houses. *Water and Environment*
704 *Journal*, 13(5), 313–318.

705 Rodriguez-Freire, L., Sierra-Alvarez, R., Root, R., Chorover, J., Field, J. A. (2014).
706 Biomineralization of arsenate to arsenic sulfides is greatly enhanced at mildly acidic conditions.
707 *Water Research*, 66, 242-253.

708 Rodriguez-Freire, L., Moore, S. E., Sierra-Alvarez, R., Root, R., Chorover, J., Field, J. A.
709 (2015). Arsenic remediation by formation of arsenic sulfide minerals in a continuous anaerobic
710 bioreactor. *Biotechnology & Bioengineering*, 113(3), 522-530.

711 Rossi-Tamisier, M., Benamar, S., Raoult, D., Fournier, P. E. (2015). Cautionary tale of using
712 16S rRNA gene sequence similarity values in identification of human-associated bacterial
713 species. *International Journal of Systematic and Evolutionary Microbiology*, 65, 1929-34.

714 Santini, J. M., Sly, L. I., Schnagl, R. D., Macy, J. M. (2000). A new chemolithoautotrophic
715 arsenite-oxidizing bacterium isolated from a gold mine: Phylogenetic, physiological, and
716 preliminary biochemical studies. *Applied and Environmental Microbiology*, 66(1), 92–97.

717 Sánchez-Andrea, I., Stams, A.J.M., Hedrich, S., Nancucheo I., Johnson D. B. (2015).
718 *Desulfosporosinus acididurans* sp. nov.: an acidophilic sulfate-reducing bacterium isolated
719 from acidic sediments. *Extremophiles*, 19, 39-47.

720 Sen, A. M., Johnson, D. B. (1999). Acidophilic sulphate-reducing bacteria: candidates for
721 bioremediation of acid mine drainage. *Process Metallurgy*, 9, 709-718.

722 Serrano, J., Leiva, E. (2017). Removal of Arsenic using acid/metal-tolerant sulfate reducing
723 bacteria: a new approach for bioremediation of high-arsenic acid mine waters. *Water*, 9(12),
724 994.

725 Simate, G. S., Ndlovu, S. (2014). Acid mine drainage: Challenges and opportunities. *Journal*
726 *of Environmental Chemical Engineering*, 2(3), 1785–1803.

727 Slyemi, D., Moinier, D., Brochier-Armanet, C., Bonnefoy, V., Johnson, D. B. (2011).
728 Characteristics of a phylogenetically ambiguous, arsenic-oxidizing *Thiomonas* sp., *Thiomonas*
729 *arsenitoxydans* strain 3AsT sp. nov. *Archives of Microbiology*, 193, 439–449.

730 Smiedja, J.A., Wilkin, R. (2003). Preservation of Sulfidic Waters Containing Dissolved As(III).
731 *Journal of Environmental Monitoring*, 6, 913-916.

732 Touzé, S., Battaglia-Brunet, F., Ignatiadis, I. (2008). Technical and Economical Assesment and
733 extrapolation of a 200-dm³ pilot bioreactor for reduction of sulphate and metals in acid mine
734 waters. *Water Air & Soil Pollution*, 187, 15-29.

735 Walters, E., Hille, A., He, M., Ochmann, C., Horn, H. (2009). Simultaneous
736 nitrification/denitrification in a biofilm airlift suspension (BAS) reactor with biodegradable
737 carrier material. *Water Research*, 43(18), 4461–4468.

738 Wang, J. W., Bejan, D., Bunce, N. J. (2003). Removal of arsenic from synthetic acid mine
739 drainage by electrochemical pH adjustment and coprecipitation with iron hydroxide,
740 *Environmental Science and Technology*, 37(19), 4500-4506.

741

742

743 **Table 1.** Characteristics of the two water samples treated in this study

Water sample	As mg.L ⁻¹	Zn mg.L ⁻¹	Fe mg.L ⁻¹	SO ₄ mg.L ⁻¹	pH
Spring S1	174	26.0	1345	3700	3.29
Spring SSR	18	4.4	307	1500	4.02

744

745

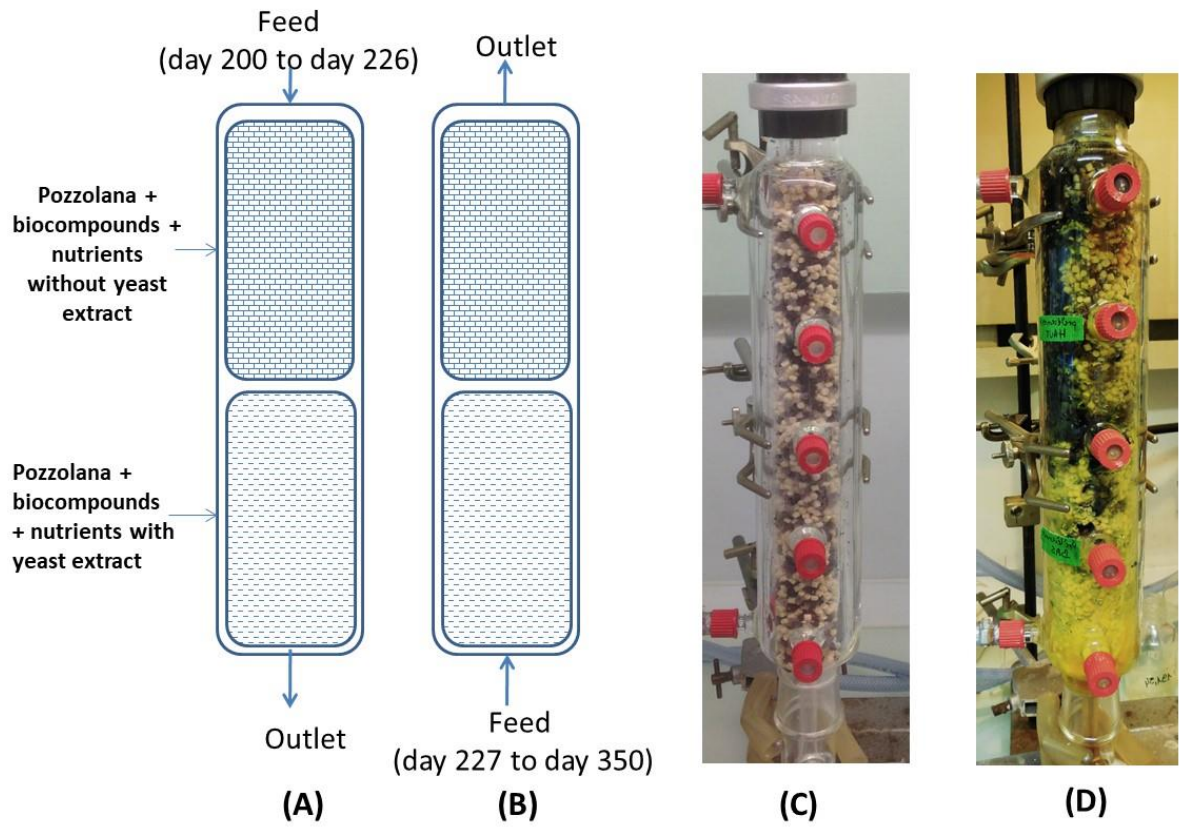


Figure 1

746

747

748

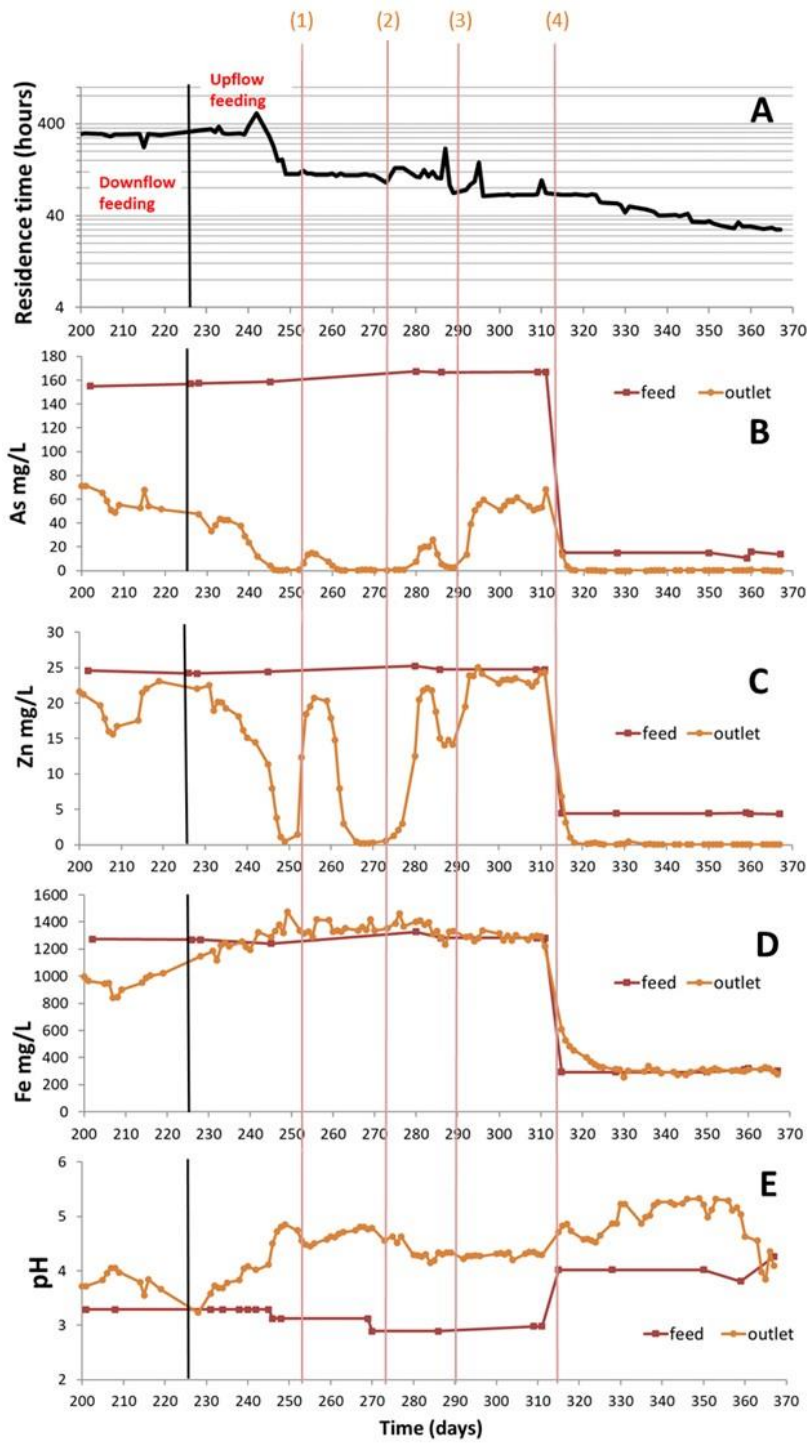


Figure 2

749

750

751

752

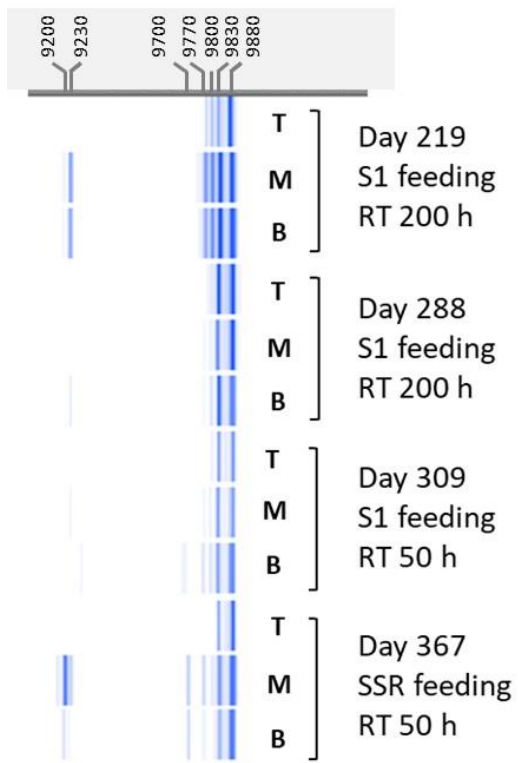


Figure 3

753

754

755

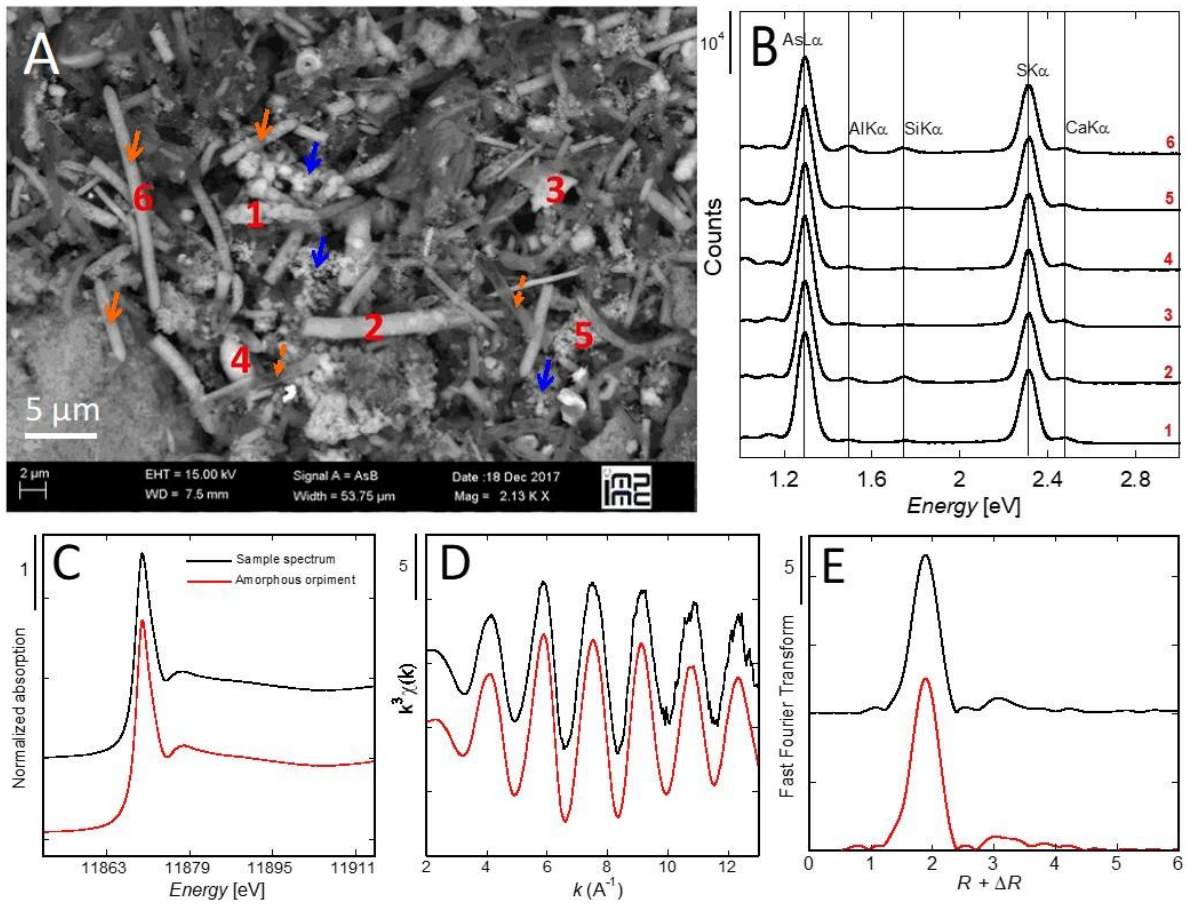


Figure 4

756

757

758

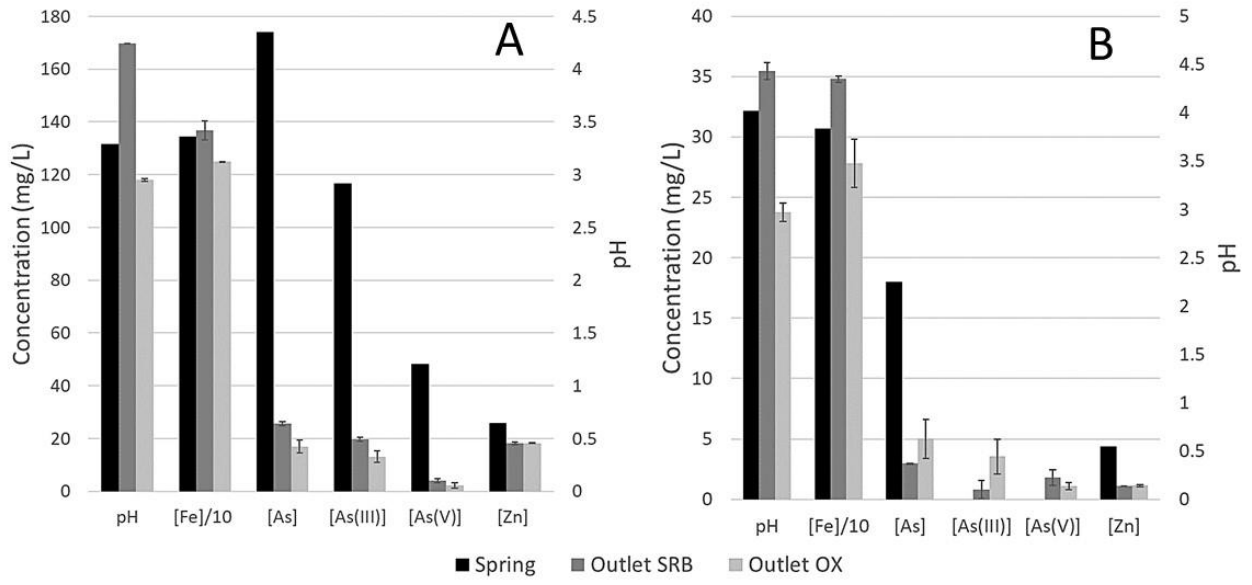


Figure 5

759

760

761

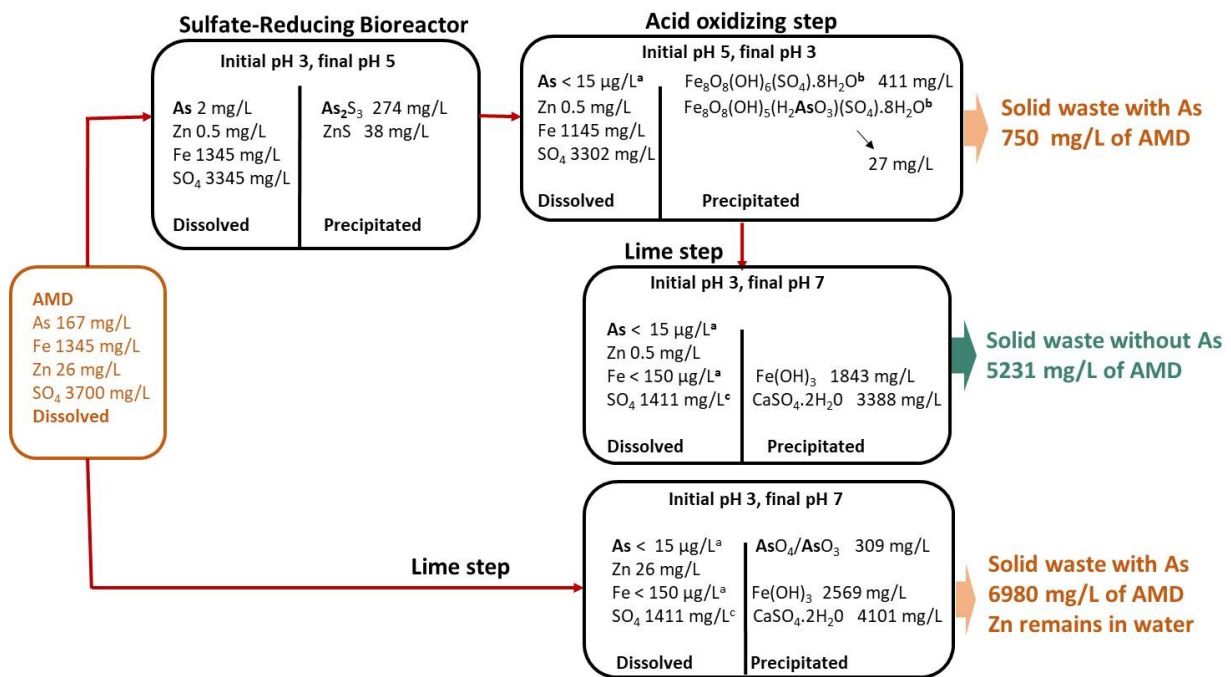


Figure 6

762

763

764

765 **Laboratory-scale bio-treatment of real arsenic-rich acid**
766 **mine drainage**

767 Battaglia-Brunet Fabienne, Casiot Corinne, Fernandez-Rojo Lidia, Hery Marina, Le Pape
768 Pierre, Tris Hafida, Morin Guillaume, Touzé Solène, Joulian Catherine

769 **Supplementary Material SM1. Composition of the basal medium**
770 **used to enrich sulfate-reducing bacteria**

771 The basal enrichment medium contained the following ingredients, per litre: K_2HPO_4 , 0.5 g ;
772 NH_4Cl , 2 g ; Na_2SO_4 , 1.4 g ; $MgSO_4$, 7 H_2O , 2 g ; glycerol, 0.5 g ; yeast extract, 1 g ; trace elements
773 solution, 1 ml. The pH of this basal solution was adjusted to 4.

774 The trace metals solution composition was the following, per litre: EDTA, 3 g ; $FeSO_4$, 7 H_2O ,
775 1.1 g ; $MnSO_4$, 65 mg ; $ZnSO_4$, 89 mg ; $NiCl_2$, 24 mg ; Na_2MoO_4 , 2 H_2O , 18 mg ; H_3BO_3 , 0.3 g ;
776 $CuCl_2$, 2 mg and $CoSO_4$, 7 H_2O , 130 mg.

777 The basal medium was heated to ebullition, then distributed in 50 mL penicillin flasks
778 equipped with rubber stoppers, flushed with N_2 , and sterilized by autoclaving 30 min at 120°C.

779

780

781

782

783

784

785

786

787

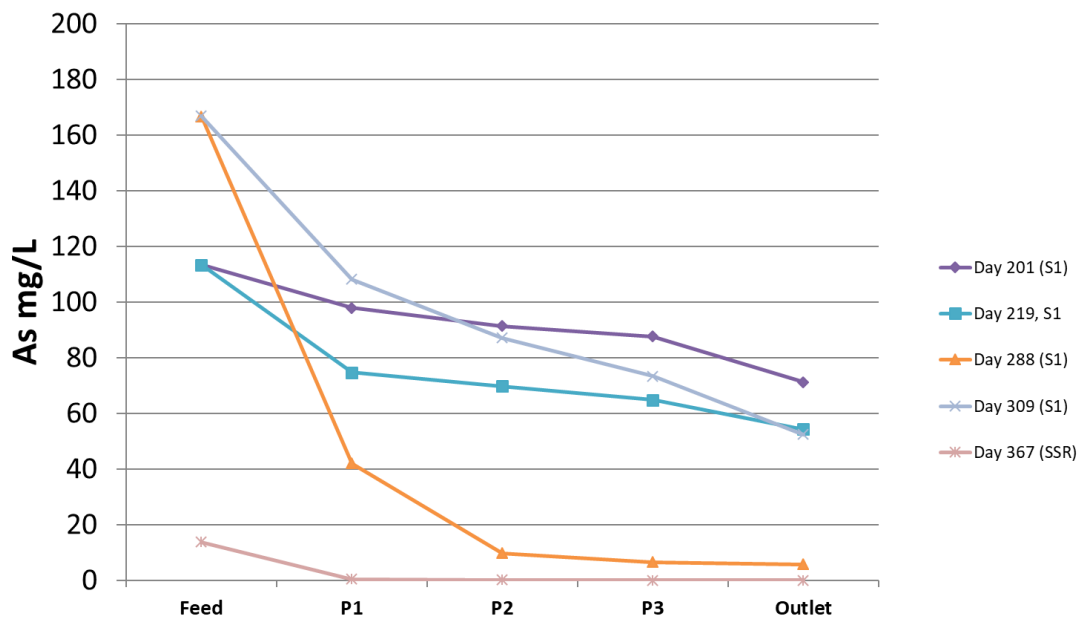
788

789

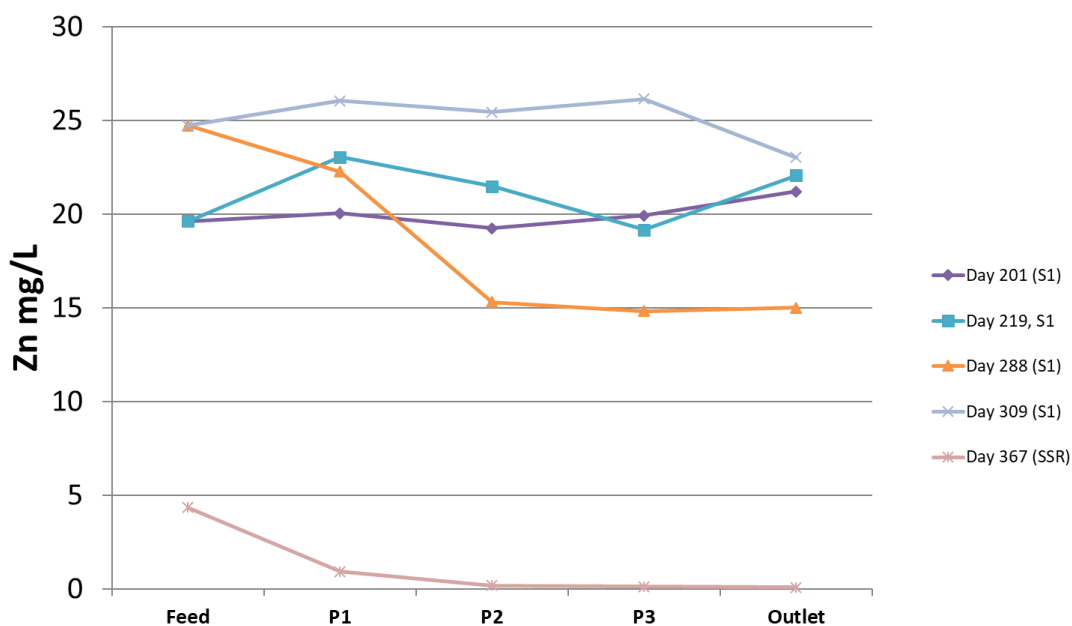
790

791

792 **Supplementary Material SM2. Profiles of As and Zn concentrations**



793



794

795

796

797

798

799

800 **Supplementary Material SM3. Acetate and total organic carbon in**
801 **the anaerobic bioreactor outlet.**

802 **Table SM3.** Acetate and total organic carbon in the anaerobic bioreactor outlet.

803

Day - condition	Acetate mg.L ⁻¹	Theoretical acetate* mg.L ⁻¹	Organic Carbon acetate mg.L ⁻¹	Total organic carbon mg.L ⁻¹
201 - S1 downflow	2.4	166	0.9	62.3
219 - S1 downflow	0.5	166	0.2	75.5
249 – S1 upflow	15.5	163	6.1	74.2
270 – S1 upflow	25.5	163	10	27.2
286 – S1 upflow	30.4	163	12	29.9
308 – S1 upflow	44.5	163	17.5	66.3
359 – SSR upflow	14.1	33	6.9	35.7
366 – SSR upflow	30.1	33	11.8	36.7

804 (*) Theoretical acetate through incomplete oxidation of glycerol in the feed water
805 according to $C_3H_8O_3 + 0.75 SO_4^{2-} + 1.5 H^+ \Rightarrow C_2H_4O_2 + CO_2 + 0.75 H_2S + 2 H_2O$

806

807

808

809

810

811

812

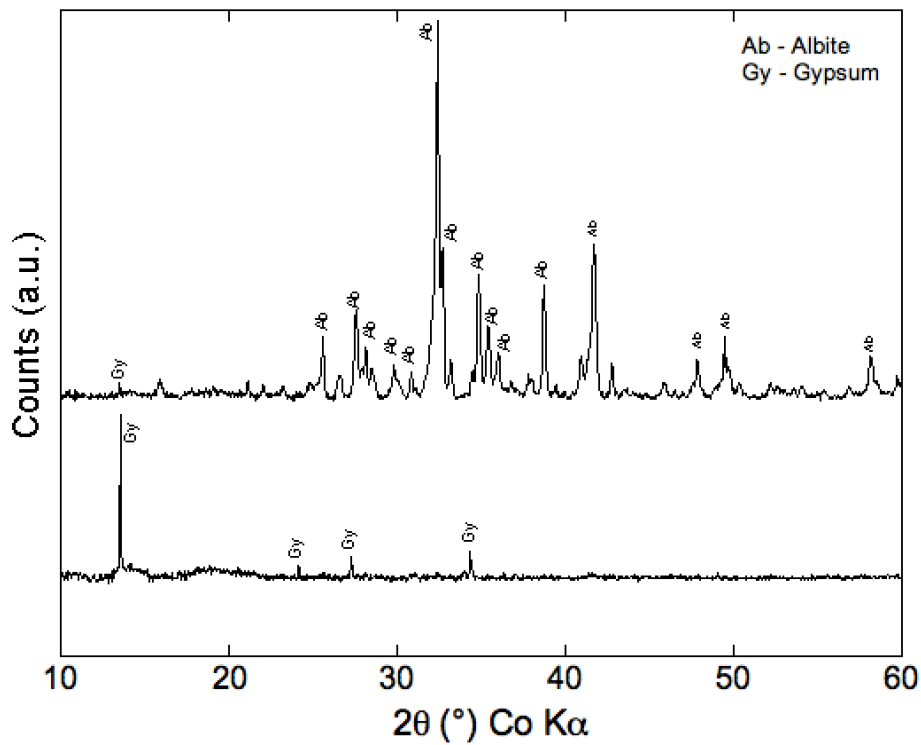
813

814

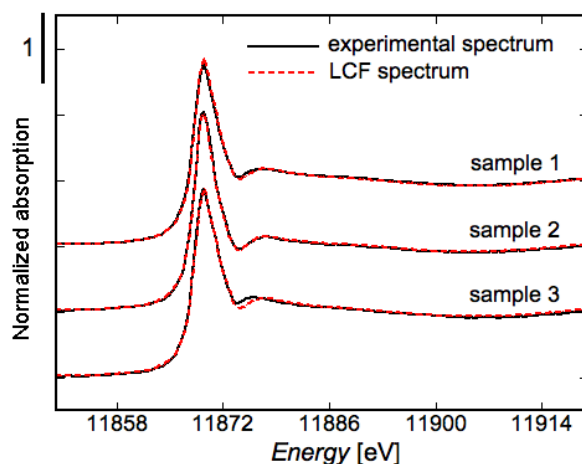
815

816 **Supplementary Material SM4. Characterization of the solid phases**
817 **sampled in the anaerobic reactor**

- 818 **Sample 1:** Black pouzzolana + yellow deposit
819 **Sample 2:** Gelatinous yellow colored material
820 **Sample 3:** Wolly black material
821
822



823 **Figure SM4-A** – X-ray diffractograms of a reacted pouzzolana grain (up) and of the yellow
824 precipitate sampled at the surface of pouzzolana grains (down). These materials were parts of
825 sample 1.
826
827



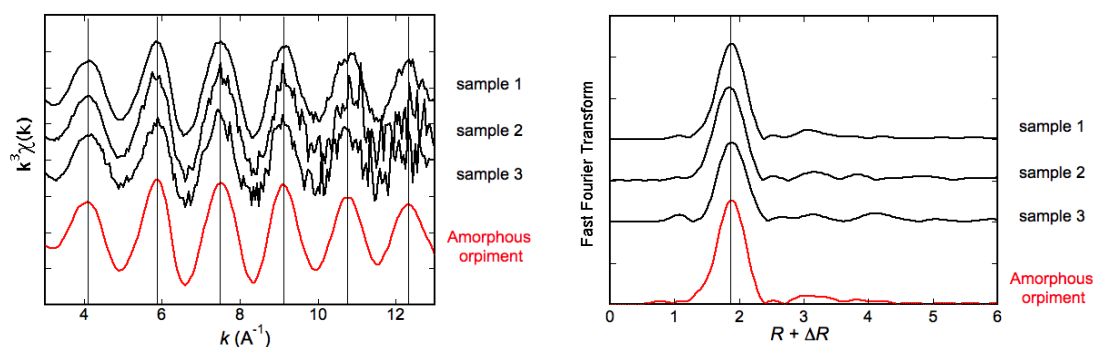
828
829 **Figure SM4-B** – X-ray Absorption Near Edge Structure (XANES) experimental spectra and linear
830 combination fits for samples 1, 2, and 3.

831
832
833
834

	amorphous orpiment	As(III)-sorbed ferrihydrite	R-factor	Red-chi2
sample 1	100	0	0.0015	0.0004
sample 2	89	13	0.003	0.00086
sample 3	90	11	0.002	0.00055

835
836
837 **Table SM4-C** – Relative contributions of As species in the experimental XANES spectra (Fig. 4)
838 by performing a linear combination fitting procedure with two reference compounds, namely
839 amorphous orpiment (As(III)-S) and arsenite-sorbed ferrihydrite (As(III)-O). R-factor and Red-
840 χ^2 are given as indicators of the quality of fits.

841



842
843 **Figure SM4-D** – Extended X-Ray Absorption Fine Structure (EXAFS) presented for the
844 experimental spectra of samples 1, 2, and 3 and for the amorphous orpiment reference
845 mineral.

846

847